Geological Structrure and Magnetics at the Burning Stone, Utah Prospect

I Geologic Data

The geologic data are taken from two geologic maps published by the U.S.G.S. (Lemmon and Morris, Lemmon, Morris and Hintze), see Figure 1. The gross features are (1) extensive exposures of Tertiary volcanics including (2) a granitic, 28.0 m.y. old pluton with (3) flanking outcrops of Paleozoic limestones, dolomites, shales and quartzites. Faults are poorly exposed but the Frisco Thrust is mapped in the Paleozoic section. There is evidence for north-south trending normal faults, and two dominantly strike-slip sets trending generally northwest-southeast and southwest-northeast. The topographic low where Highway 93 enters the Wah Wah valley appears to be an intersection of the strike-slip faults.

II Magnetic Interpretation

A. Data

Two sets of aeromagnetic data are available. Set one was flown at a constant barametric altitude of 9000' in 1963. The survey was flown along east-west flight lines usually 1 mile apart with no tie lines (U.S.G.S.) see Figure 2. The flight line spacing of this data limits horizontal resolution in the north south direction to about 1 mile at best. Set two was flown for AMAX during 1971 at a mean terrain clearance of 450 ft. The survey was flown along north-south flight lines about 1500 ft apart with tie lines. (See Figure 3) Because the coverage of the low level data is restricted to the exposed pluton and its flanks, the high level data were chosen to digitize and model. The reader should be aware that the variable flight line spacing of this data severly limits resolution in certain areas of the map.

B. Magnetic Properties

It was assumed Natural Remanent Magnetization (NRM) could be ignored in this area. This assumption is based on the absence of (NRM) measurements and of magnetic lows possibly caused by reversed NRM directions. Significant magnetic susceptibilities were measured from 19 samples of the intrusive rocks (Schmoker 1972). These susceptibilities ranged from 0.00237 to 0.00440 emu/cc with an average of 0.00345 emu/cc. Susceptibility measured from 4 skarn-contact samples averaged 0.1 emu/cc. Samples of alluvium and Tertiary volcanics had an average susceptibility of 0.00020 emu/cc. Five Paleozoic sedimentary rock samples had an average susceptibility of 0.00009 emu/cc. The local inclination, declination and intensity of the earths magnetic field are as 16^{o}, 64^{o} and 54000 gammas respectively.

C. Regional Magnetic Anomaly

A regional anomaly was subtracted from the observed data to produce a residual anomaly map. The procedure for determining a regional involves choosing the numerical technique and identifying and applying the geological and geophysical constraints. The regional used in this report was calculated from a two body magnetic model. The following constraints were applied.

Geologic constraints: The geologic explanation is that the regional magnetic anomaly is caused by a Tertiary batholithic pluton (Schmoker 1972). Above the pluton are cupolas which correspond to outcrops of quartz monzonite to granodiorite. The granitic batholith has an irregular floor several kilometers deep. Cupolas generally enlarge downward and connect with the main batholith. The shape of the floor and sides of the batholith is partially controlled by regional faults related to crustal (east-west) extension during the Tertiary. The floor and cupolas generally intrude a thick sequence of Paleozoic basement rocks which are relatively non-magnetic.

Geophysical constraints: Based on regional gradients observed in the data the regional anomaly was considered to have three causitive elements (features AAA, BBB and CCC on Figure 2). They are: (1) the generally east-west directed north edge of the pluton; (2) a westward stepdown into the Wah Wah valley, striking north-south; (3) a northwest step down across the Wah Wah valley, striking northeast-southwest.

Observed and calculated data are shown along a north-south profile (Figure 4). With a susceptibility contrast of .00150 cgs the regional model suggests a 8 km thick pluton with a floor at about 1.2 km (4000 ft) below sea level in the prospect area. This is similar to the regional picture given by Schmoker (1971). On the north-south profile the calculated regional is excessive at the south end of the profile. Consequently 20 to 90 gammas too much was removed along the south edge of the observed data. This part of the ap is not critical to the interpretation.

D. Residual Anomaly

The primary area of interest, around the thermal anomaly, is shown in Figure 2. Within this 210 km^2 area data was digitized every 500 meters and computer contoured (Figure 5). A regional was calculated at the same data locations and computer contoured (Figure 6). This regional was subtracted from the observed gridded data to give the residual magnetic anomaly (Figure 7).

The residual and the observed data are very similar. Six closed magnetic anomalies are present on the residual map. Their causitive sources are as follows (see letters Figure 7):

Anomaly A: Neglecting contact skarns and breccia pipes the large magnetic high over the San Francisco Mtns. is caused by a cupola of granodiorite deroofed and exposed.

Anomaly B: Located over the Big Wash drainage this east-west elongate magnetic high has no apparent geologic or topographic expression. It does connect to the east with a series of magnetic highs over exposed granitic rocks and is probably caused by a unexposed cupola.

Anomaly C: This attached magnetic high occurs over extensive outcrops of Horn Silver andesite. It seems reasonable to speculate a duel source. The shallow source is probably the andesite and the deeper source seems related to anomaly B.

Anomaly D: Centered between two weaker magnetic lows, this low occurs over outcrops of Pakoon Dolomite and Callville limestone. It seems likely that these Paleozoic basement rocks cause this low.

Anomalies E and F: These magnetic lows occur close to outcrops of Tertiary volcanics and they should be present beneath the lows. The most likely cause is hydrothermal alteration but it could be a reversed remanent magnetization direction.

Two saddle shaped magnetic highs separate the three magnetic lows. The western high occurs over a peninsula shaped outcrop of Horn Silver andesite which is probably the causitive source. The eastern magnetic high appears to be related to the Squaw Peak quartz latite. Squaw Peak, a possible extrusive center, is located on the south side of this high.

E. Operations and Observations

Rational: Four operations were applied to the residual magnetic data to resolve faults and contacts and to help in positioning prisms in the modeling process. The residual data was upward continued to help indicate the relative depth extent of anomalies. The data was downward continued to improve the definition of weak anomalies. Rotation to the pole (RTP) was used to remove the distorting effects of the non-vertical earth's magnetic field. The second vertical derivative of the RTP data was used to delineate the boundaries of the causitive magnetic bodies. This derivative operation enhances the near surface geological effects and subdues the effects of deeper sources.

Procedure: Two procedures were necessary to prepare the data for the above operations. A constant of 2400 gammas was removed from the data and a 10-km wide half-cosine-tapered border of data was added around the 2400-gamma-shifted-residual data. The shifted extended data was then Fourier transformed, multiplied by the appropriate operator and inverse Fourier transformed. A U. S. Geol. Survey computer program written by Richard Blakely was used to rotate to pole and continue the data. The border around the shifted-extended-operated-on data is removed and the data was contoured.

Observations: The residual-shifted magnetic data upward continued 500, 1000, 1500 meters are shown in figure 8, 9 and 10. As the data is progressively upward continued there is a suggestion of a weak magnetic source below Squaw Peak between anomalies A and B. Magnetic anomaly C lost closure on figure 8 and is hard to resolve from anomaly B in figure 9. The implication is that anomaly C and the western saddle shaped magnetic high have a shallow source with a depth extent of at least 500 meters but probably not 1000 meters. It also suggests the deep source of anomaly C and the causitive source of anomaly B are the same, namely granitic rocks from the pluton. Following the same line of reasoning for anomaly D. The Paleozoic basement rocks below anomaly D extend downward at least 1000 meters but probably not 1500 meters. Anomalies E and F open up but persist in the upward-continued-200 meters data indicating they have sources with a depth extent of at least 1500 meters. Anomaly F appears to have the deeper source. Because anomaly E is located directly over the polarization low associated with anomaly B its depth extent could be less than 1500 meters.

The residual-shifted magnetic data was downward continued 300 meters (Figure 11). The coarse flight line spacing makes this operation somewhat questionable. Two observations are made. Anomalies E and F still lack resolution in their centers. Weak but positive support for the hydrothermal alteration explanation. The two saddle shaped highs widen more sharply to the south indicating that their shallow sources are in that direction.

The residual-shifted magnetic data was rotated to pole. The magnetic inclination was rotated from 64^{0} tp 90^{0} and the magnetic delineation was rotated from 16^{0} tp 0^{0} (Figure 12). Anomalies generally moved north 75 to 2000 meters and east 250 to 750 meters. This movement places anomalies A, C, D and the western saddle shaped high more toward the center of the granodiorite, Horn Silver andesite and Paleozoic limestone outcrops. Anomaly E is now narrow and opens to the west. This severe change is partly due to the annihilation of the polarization law which was present along the northeast side of anomaly B. On the geologic map there are faults along the axis of anomaly E suggesting some credability to the anomaly shape.

The second vertical derivative was calculated for the rotated-to-pole data and the zero contour was chosen as the best indicator of magnetic boundaries (Figure 13). This map was superimposed over the rotated to pole map, the geologic map, the drape-flown aeromagnetic map and the original constant barometric aeromagnetic map. With attention to the flight line locations, linear trends were chosen and placed on an interpretation overlay (Figure 14). A pattern of trends emerge which is related to the fault patterns caused by east-west crustal extension during the Tertiary. This pattern includes northwest-southeast trends (features 1 and 5) which correspond to right-laterial wrench fauts. It also includes trends corresponding with northeast-southwest striking left-laterial-strike-slip faults (features 2, 3, and 4), north-south normal faults (feature 6) and east-west reverse or thrust faults (feature 7). The strike slip faults strongly influence the direction of streams draining into the Wah Wah valley. They seem to have controlled the shape of the Horn Silver andesite and granodiorite exposures.

F. Residual 3-D Magnetic Model

Rational: The model study was done mainly to resolve the shape of the granodiorite body along its south and west margins and to resolve the thickness and shape of the Horn Silver andesite south of the granodiorite.

Procedure: The residual aeromagnetic data (Figure 7) was used to develop the 3-dimensional magnetic model. Modelling is an iterative process. A first guess model is cauculated and iteratively improved by adding and adjusting prisms until the difference between the residual data and the calculated data are "acceptable". The computer program uses the Talwani (1965) equation intergrated in the vertical direction to calculate the total magnetic field of a polygonal right prism.

Results: The model is shown in Figure 15 and consists of 9 prisms. The model may be divided into the north four prisms and the south five prisms. The north four prisms represent the granodiorite cupola. They indicate it has 1750 meters (5900 ft) of relief along the near vertical east side, 3250 meters (10700 ft) of relief along the westward dipping Wah Wah Valley side and 3250 meters of relief along the north and south sides. Much of the relief especially along the north, south and east sides is probably due to faulting. The two elongate northeast and southeast extensions on the top two prisms suggest the granodiorite emplacement was directed along preintrusion faults striking in those directions. Prism five indicates the pediment covering the granodiorite 1500 meters west of the outcrop is about 100 meters thick. It also suggests immediately west of this shallow cover the granodiorite is down dropped along normal faults. The upper granodiorite contact seems to deepen rapidly beneath the Paleozoic rocks exosed along south side of the intrusion.

The south half of the model contains five prisms, three of which represent granitic intrusive rocks. These three prisms indicate the source of anomaly B is possibly within 300 meters of the surface. In the south model the west sides of the prisms are parallel to the northeast-trending strike slip faults. This suggests either preintrusion fault control or post intrusion down faulting to the west. The model indicates 1700 meter (5680 ft) of relief along the east, west and south sides of this possible intrusion. There is no topograhic expression of this relief as there was for the exposed cupola to the north. This suggests the source of anomaly B is probably covered with Tertiary ignimbrites and alluvium.

One prism of the south group represents the Horn Silver andesite. It indicates the andesite exposed southwest of Squaw Peak is about 500 meters (1640 ft) thick. The elongate prism shape suggests the eruptive center was probably linear and aligned with the northeast trending left lateral faults. The Horn Silver andesite north of Squaw Peak has little to no magnetic expression in the data which suggests it is either altered or very thin.

One prism represents the Quartz Latite of Squaw Peak. This 500 meter thick prism indicates the exposed extrusive pile sits on top of its eruptive center.

The total field intensity calculated over this model is shown in figure 16. This should be compared with the DC-shifted residual data shown in figure 7. To aid in this comparison the calculated data were subtracted from the residual data. This residual is shown in figure 17. The 200 gamma contour corresponds to the zero residual. The largest residuals occur along the north and east sides of the upper prisms representing the exposed cupola. This pattern of a central low surrounded by a magnetic high has several ipossible explanations. Some of this pattern is caused by ficticious data between flight lines. Hopefully most of the pattern is caused by strong shallow magnetic sources along the granodiorite contact which were not accounted for in the model. The outline of the granodiorite contact seems to support this explanation.

This residual also indicates the model is 40 to 100 gammas deficient over anomaly B and 20 to 40 gammas excessive over the three connected magnetic lows. Two segments of a northeast to southwest trending 60 gamma gradient are present in this residual data. There segments correspond with aligned fault segments on the geologic map and aligned linear trends on the second derivation of the rotated to pole data. The south segment indicates a deficiency of magnetic material in the model along the west side of anomaly B. The north segment indicates either a deficiency along the east side of anomaly A or an excess east of Highway 93.

G. Conclusions and Recommendations

The major conclusion is that the processes of horizontal extension and intrusion during the Tertiary can explain all the structure indicated by the magnetic interpretation. The northwest-trending strike-slip faults which seem to have large dip slip displacements seem to influence the shape of the thermal anomaly. The east-west series of connected magnetic lows probably represent a relect hydrothermal system in which east-west faulting possibly controlled fluid circulation. The fault intersection pattern and the geometry and size of the pluton suggest some deep fluid circulation mechanism as the source of the thermal anomaly.

A dipole-dipole profile is located over each of the three connected magnetic lows. Models of these profiles would be helpful in constructing a geologic cross section. If the thermal well data were downward continued it could help resolve the faults which influence the shallow thermal circulation. Some gravity profiles should help resolve the pediment thickness.

figure 1

geologic map

E REPORT 79-724

FRISCO QUADRANGLE
UTAH–BEAVER CO.
15 MINUTE SERIES (TOPOGRAPHIC)

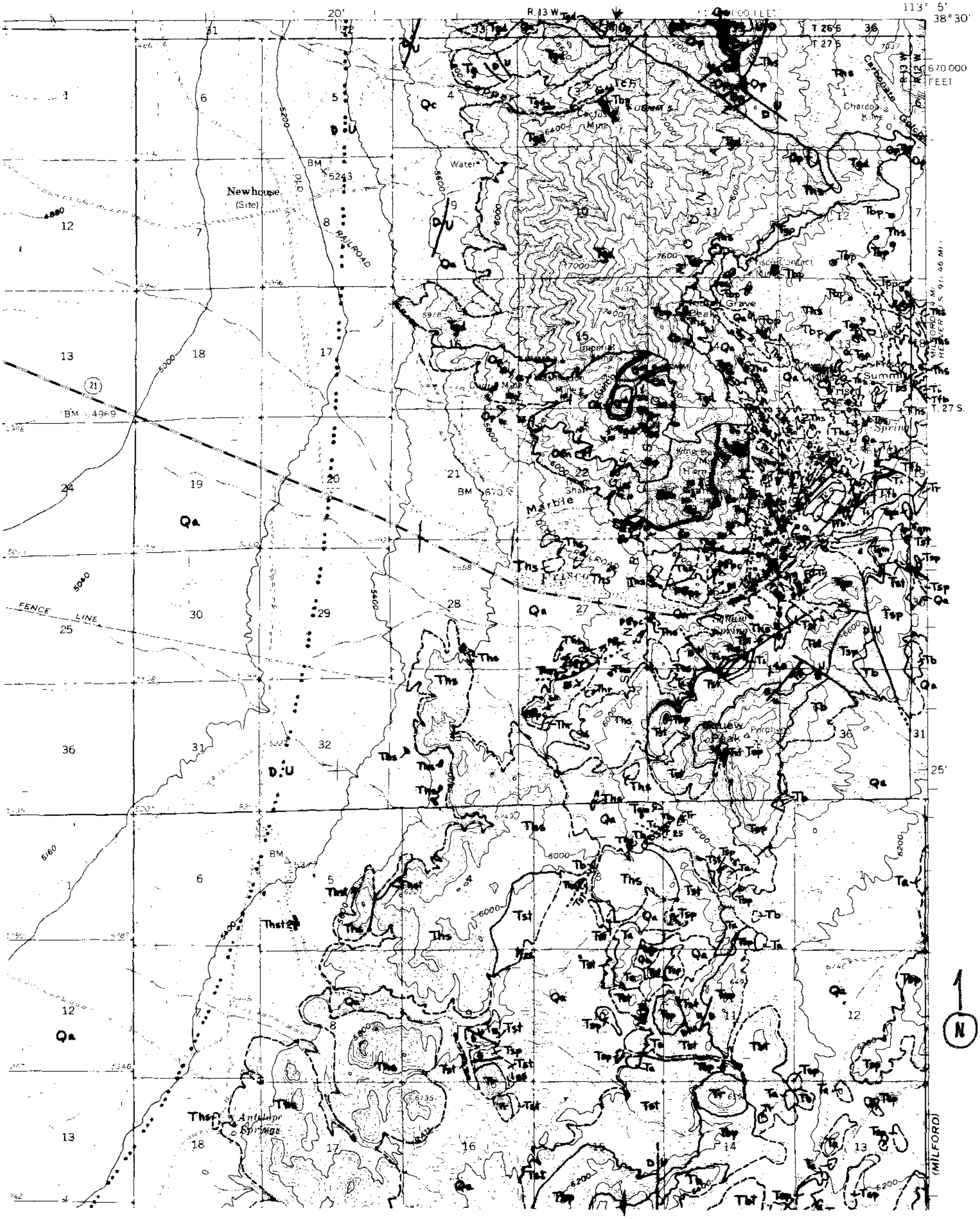

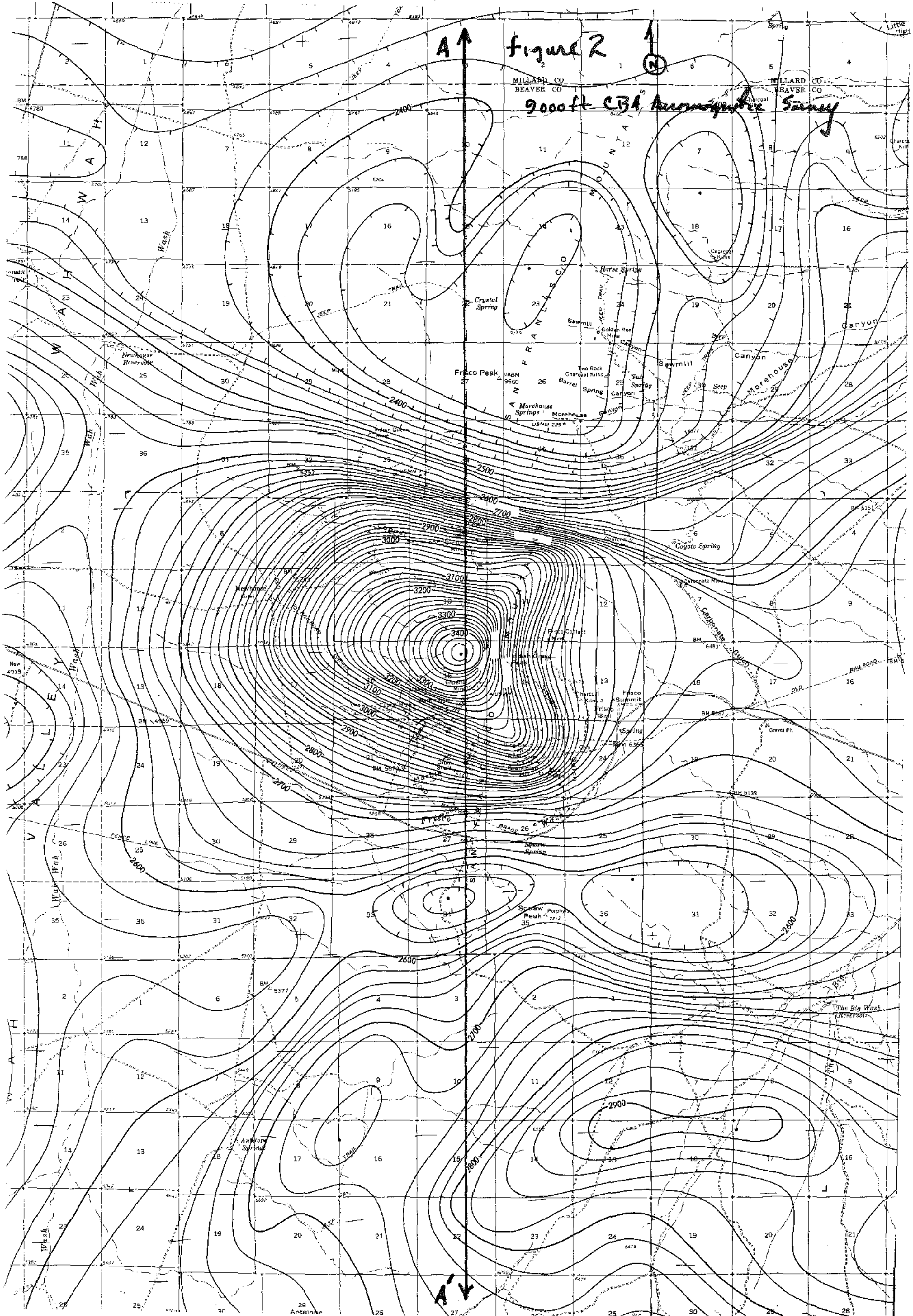

A
A'
figure 2
9000 ft CBA Aeromagnetic Survey
MILLARD CO
BEAVER CO
Frisco Peak
Crystal Spring
Horse Spring
Sawmill
Golden Reef Mine
Sawmill Canyon
Morehouse Canyon
Two Rock Charcoal Kilns
Barrel Spring
Tub Spring
Morehouse Springs
Morehouse
Newhouse Reservoir
Indian Queen Mine
Coyote Spring
Carbonate Mine
Carbonate Gulch
Newhouse
Frisco Contact Mine
Frisco Summit
Frisco
Squaw Spring
Squaw Peak
Gravel Pit
The Big Wash Reservoir
Antelope Spring
Antelope
Wah Wah Wash
2400
2500
2600
2700
2800
2900
3000
3100
3200
3300
3400

figure 3

450 ft drape flown aeromag Survey

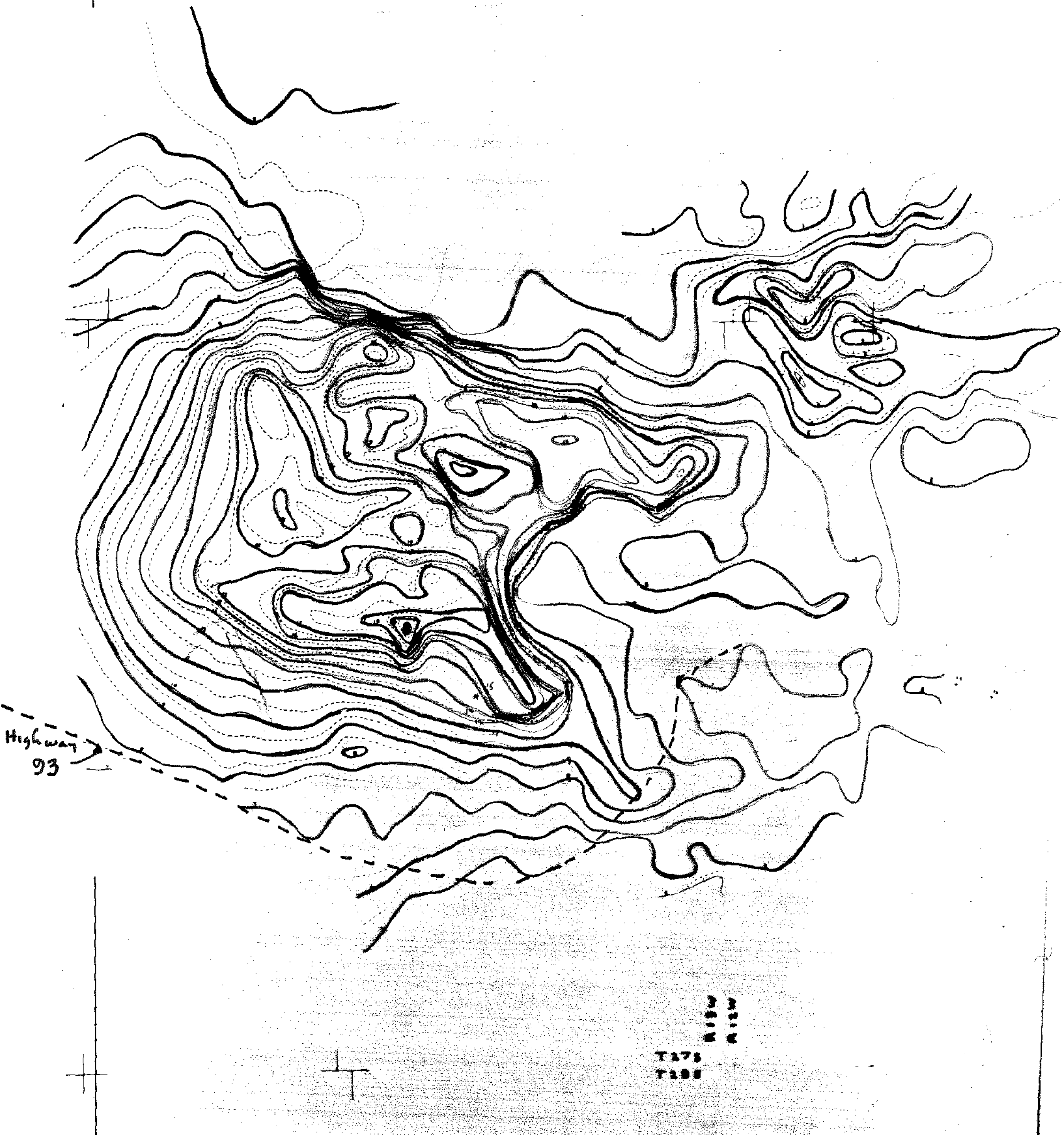

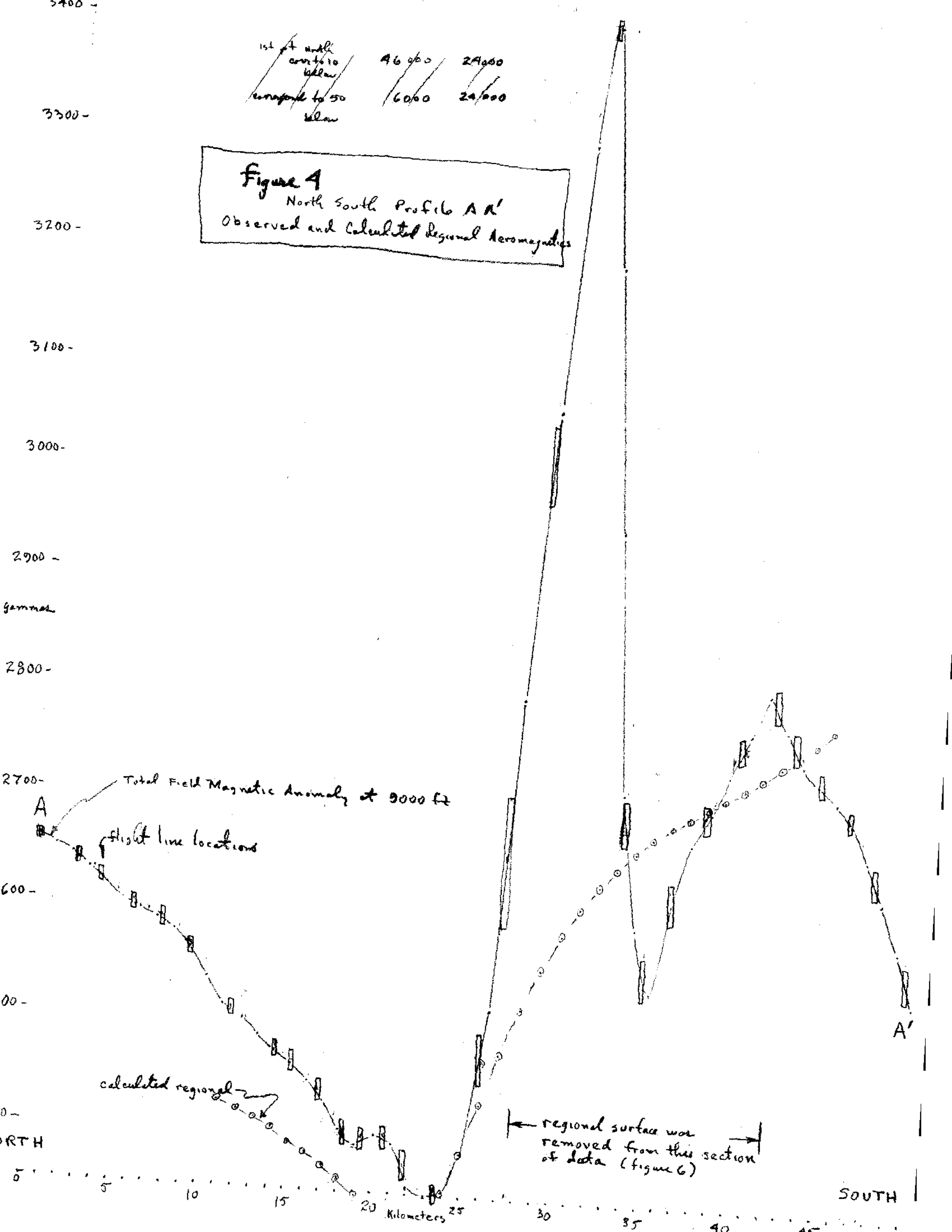

Figure 4
North South Profile A A'
Observed and Calculated Regional Aeromagnetics

JOB-ID: BERKMAN /PROGRAM NAME: CALCON /PPN[27100,02700]/DATE AND TIME: 8-Feb-82 17:13
JOB-ID: BERKMAN /PROGRAM NAME: CALCON /PPN[27100,02700]/DATE AND TIME: 8-Feb-82 17:13

BURNING STONE 125M. GRID

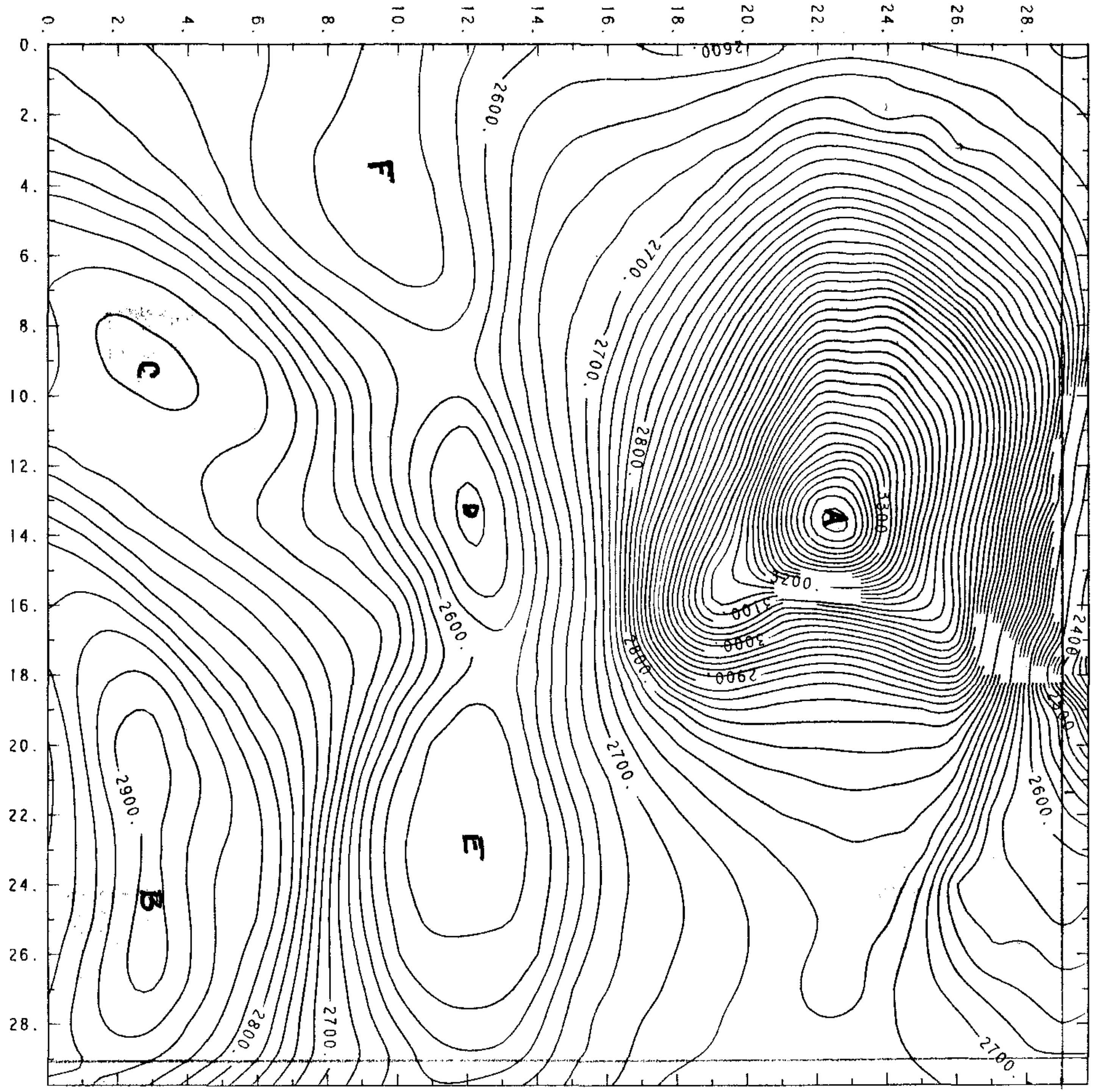

figure 5

figure 5

figure 6

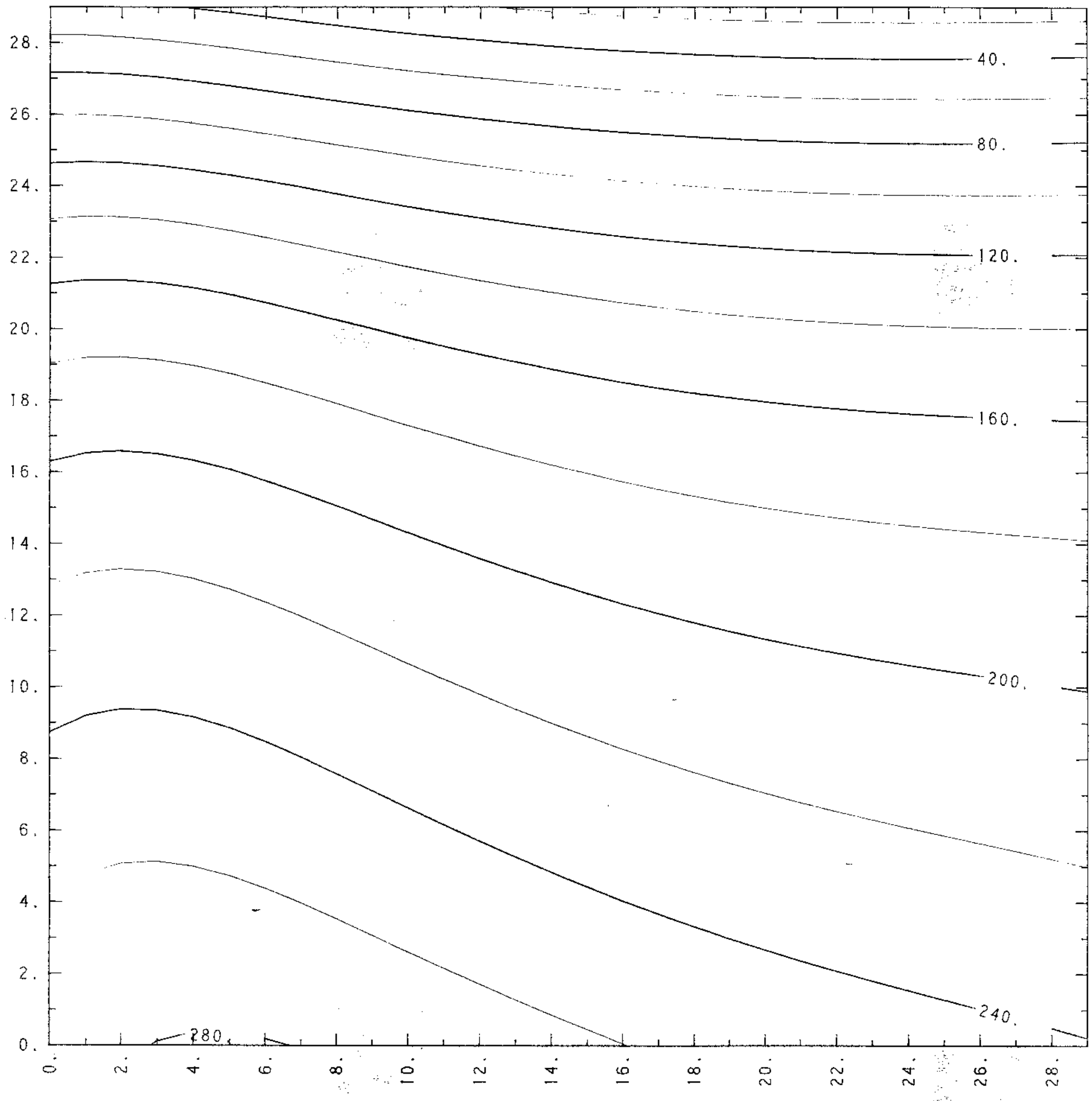

BURNING STONE REG. MAG. MODEL

figure 7

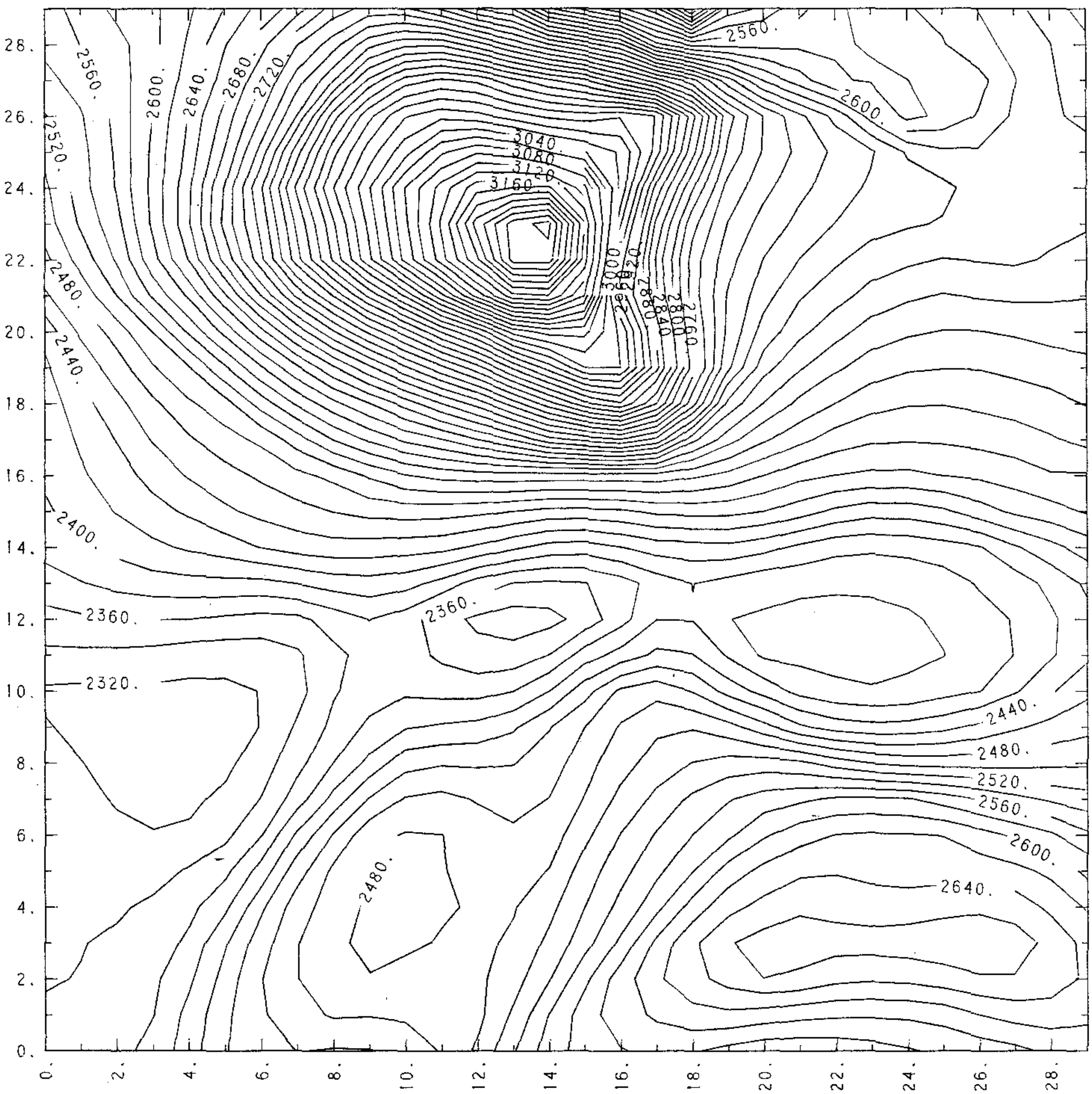

BURNING STONE RESIDUAL AEROMAG.

JOB-ID: BERKMAN /PROGRAM NAME: CALCON /PPN[27100,02700]/DATE AND TIME: 18-Feb-82 14:18

JOB-ID:BERKMAN /PROGRAM NAME:CALCON /PPN[27100,02700]/DATE AND TIME:25-Feb-82 15:07

JOB-ID:BERKMAN /PROGRAM NAME:CALCON /PPN[27100,02700]/DATE AND TIME:25-Feb-82 15:07

BURNING STONE RES AEROMAG UPWD CCNT 5000M

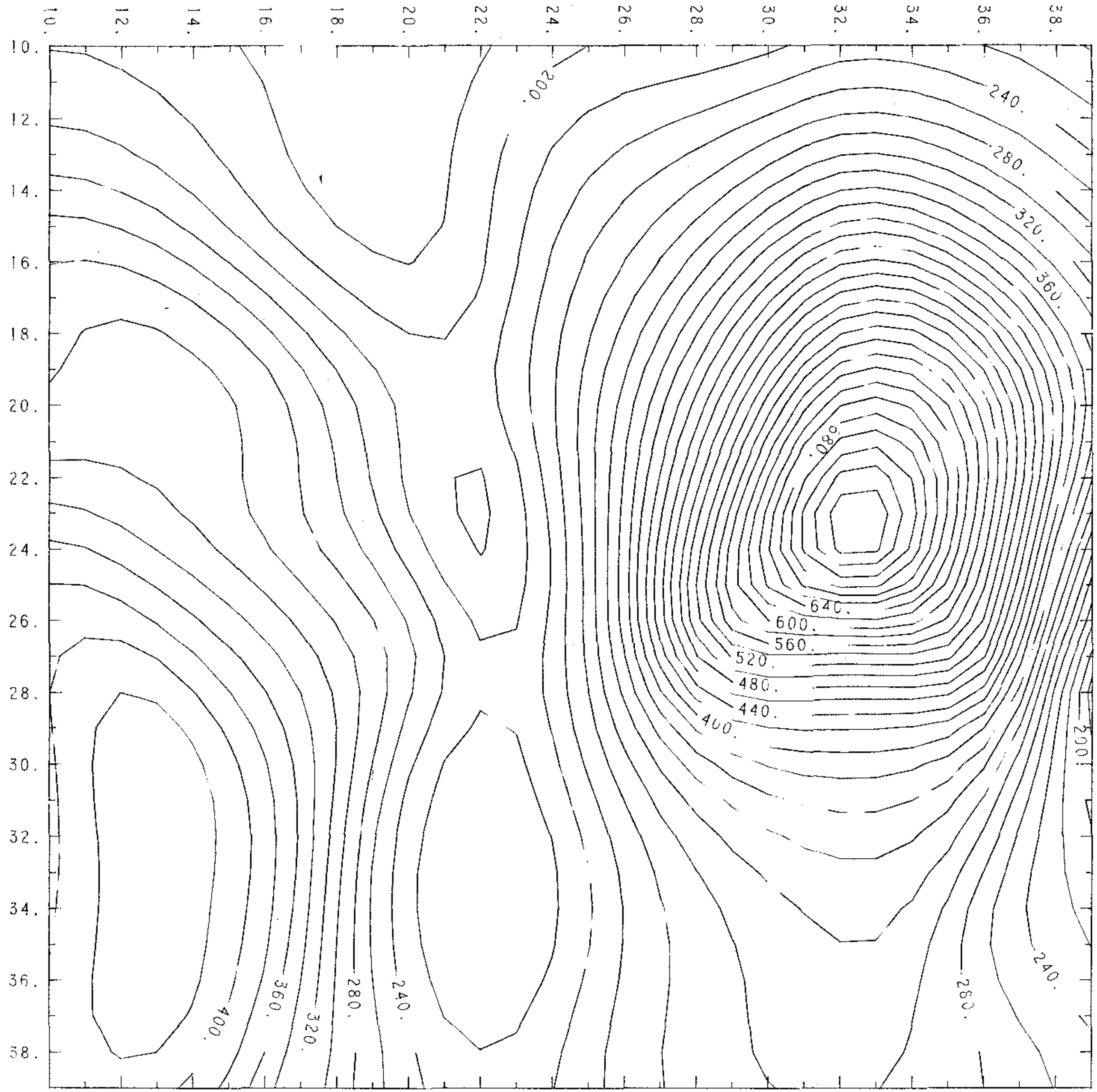

figure 8

JOB-ID:BERKMAN /PROGRAM NAME:CALCON /PPHE27100,027003/DATE AND TIME:25-Feb-82 15:21
JOB-ID:BERKMAN /PROGRAM NAME:CALCON /PPHE27100,027003/DATE AND TIME:25-Feb-82 15:21

BURNING STONE RES AEROMAG UPWF CONT 1KM

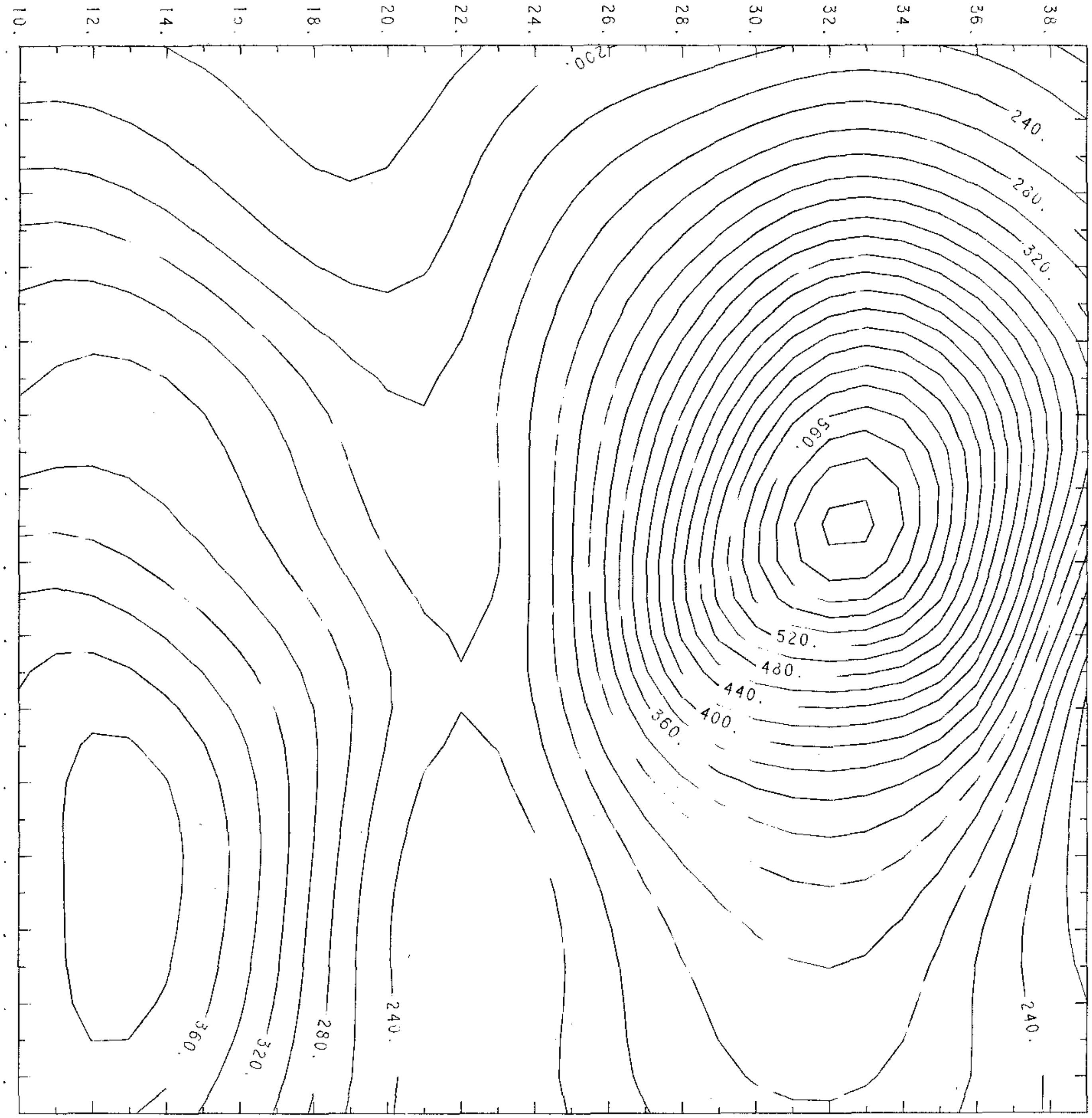

Figure 9

JOB-ID:BERKMAN /PROGRAM NAME:CALCON /IPN[27100,02700]/DATE AND TIME: 4-Mar-82 11:59
JOB-ID:BERKMAN /PROGRAM NAME:CALCON /PPN[27100,02700]/DATE AND TIME: 4-Mar-82 11:59

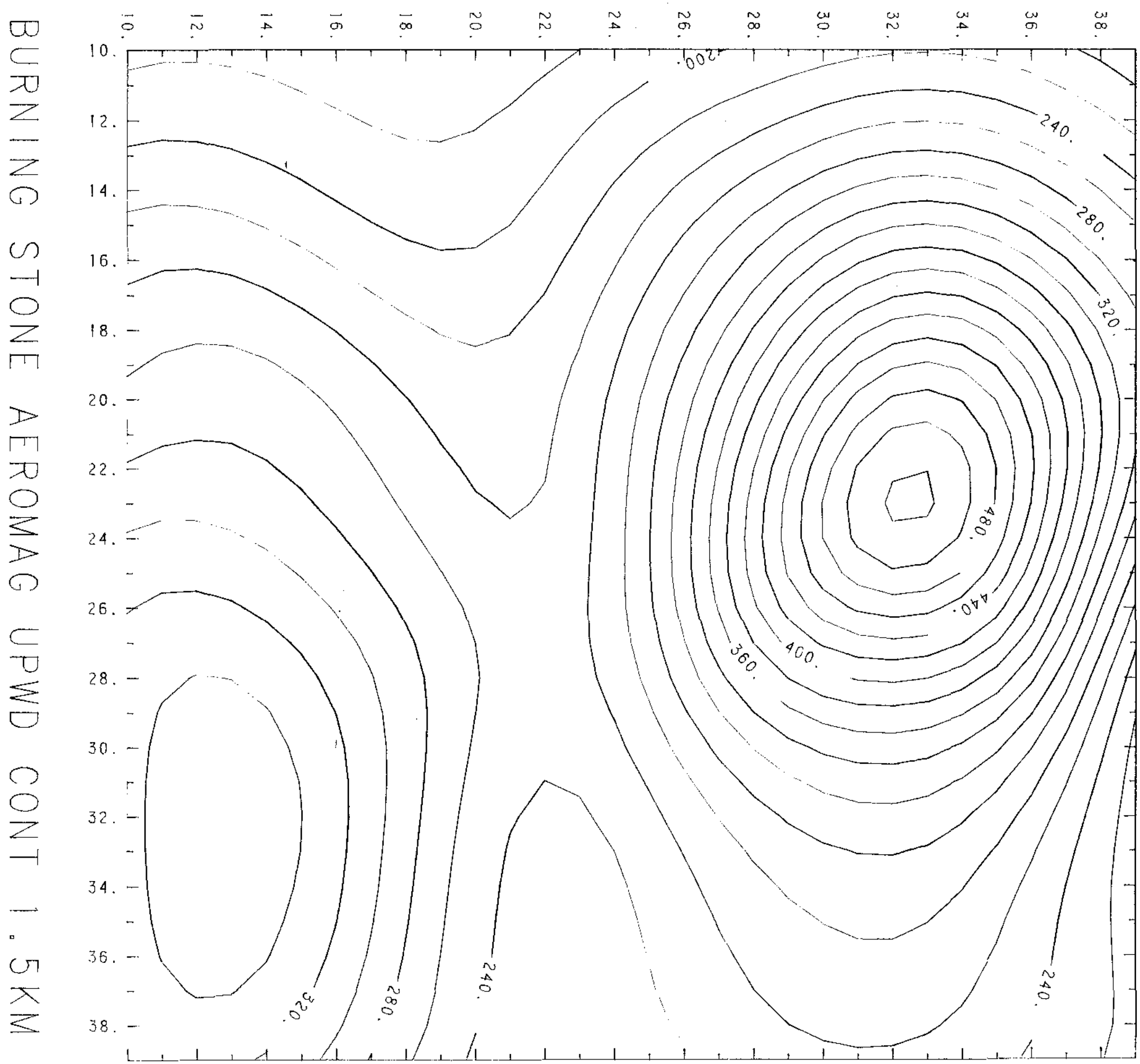

figure 10

Figure 11

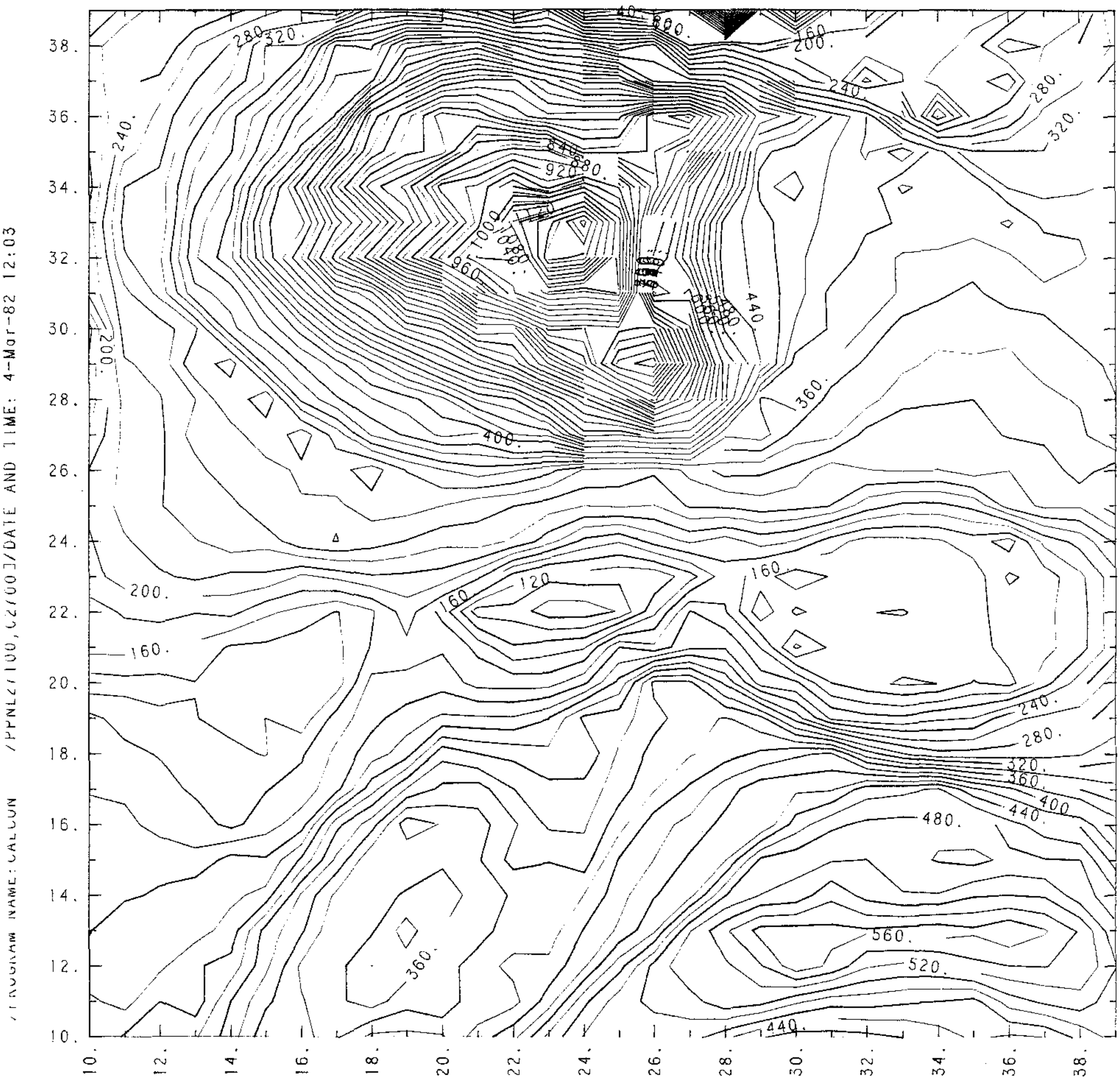

BURNING STONE AEROMAG DWND CONT 300M

figure 12

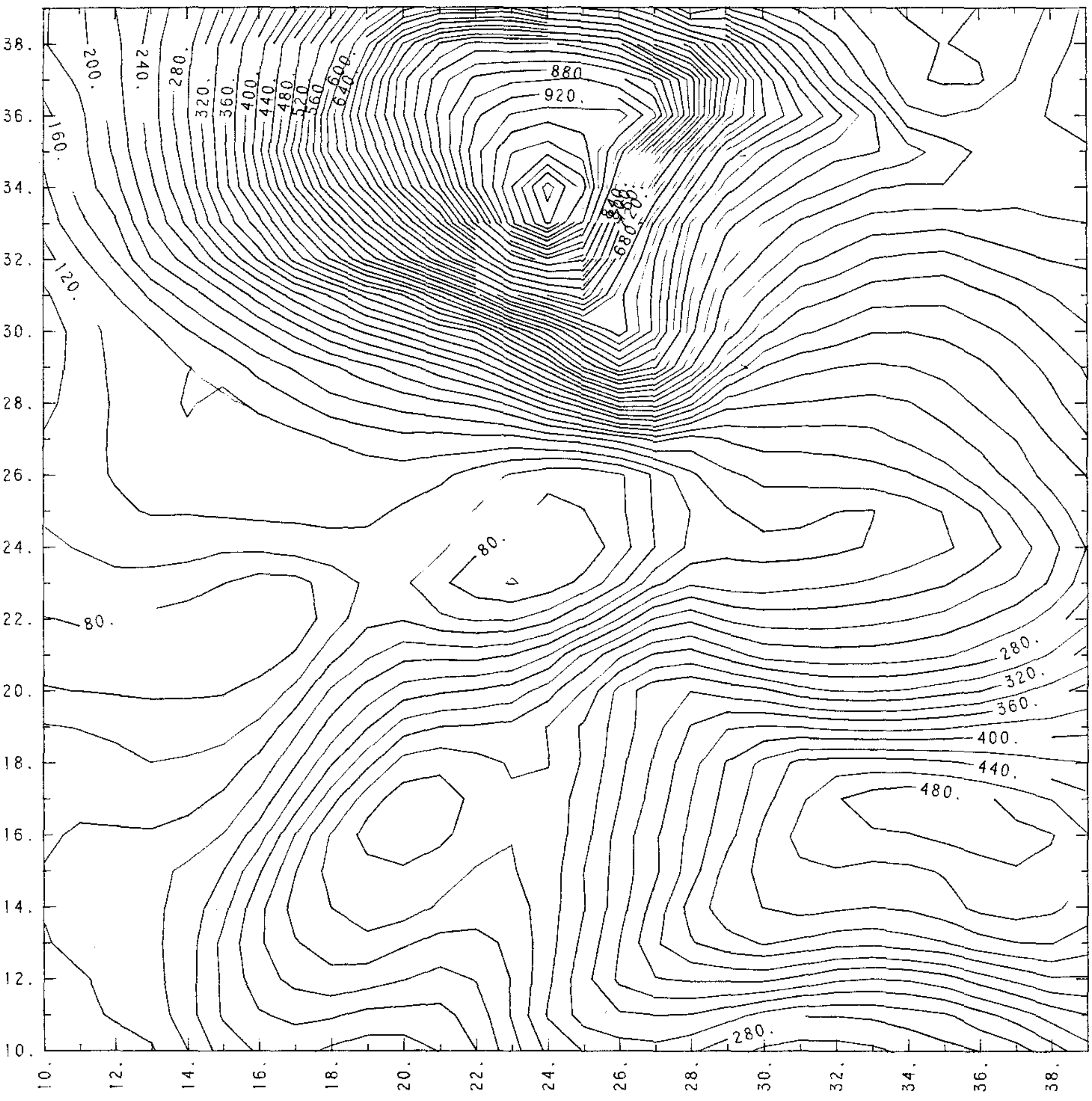

BURNING STONE RES AEROMAG ROTA TO POLE

figure 13

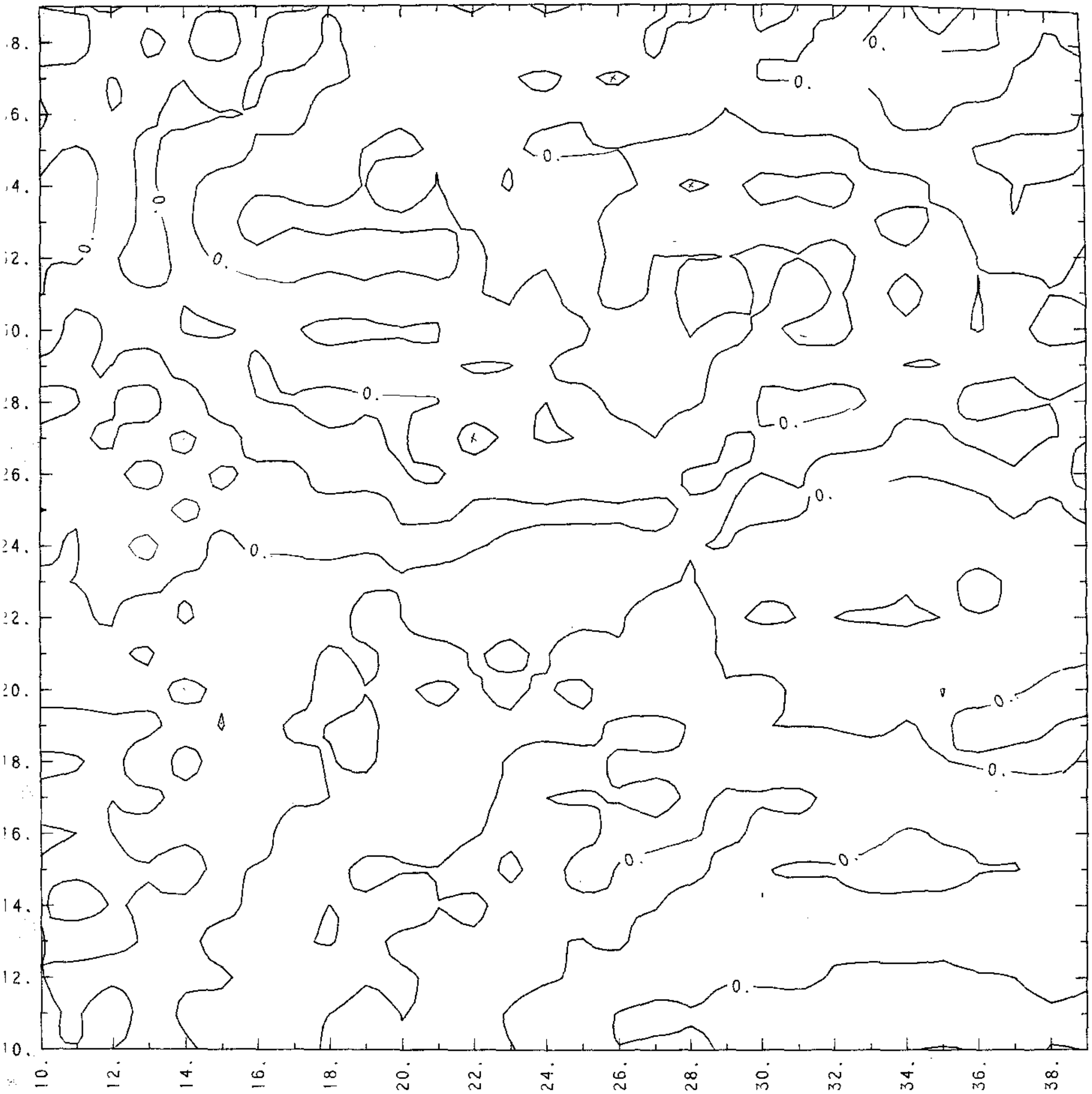

BURNING STONE RES AEROMAG ROTA TO POLE
SECOND VERTICAL DERIVATIVE
ZERO CONTOUR ONLY

figure 14

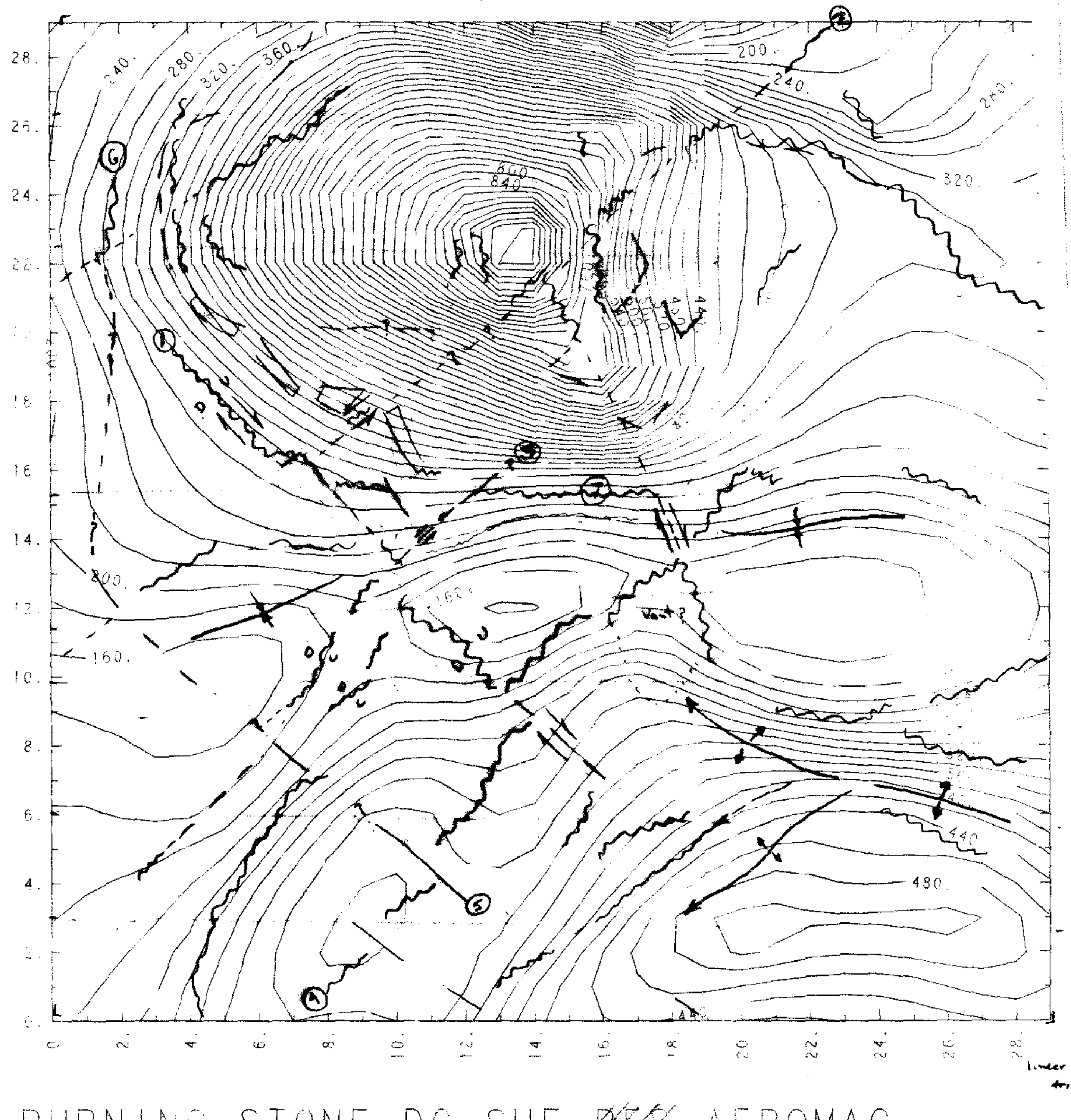

BURNING STONE DC SHF ~~RES~~ AEROMAG

figure 15

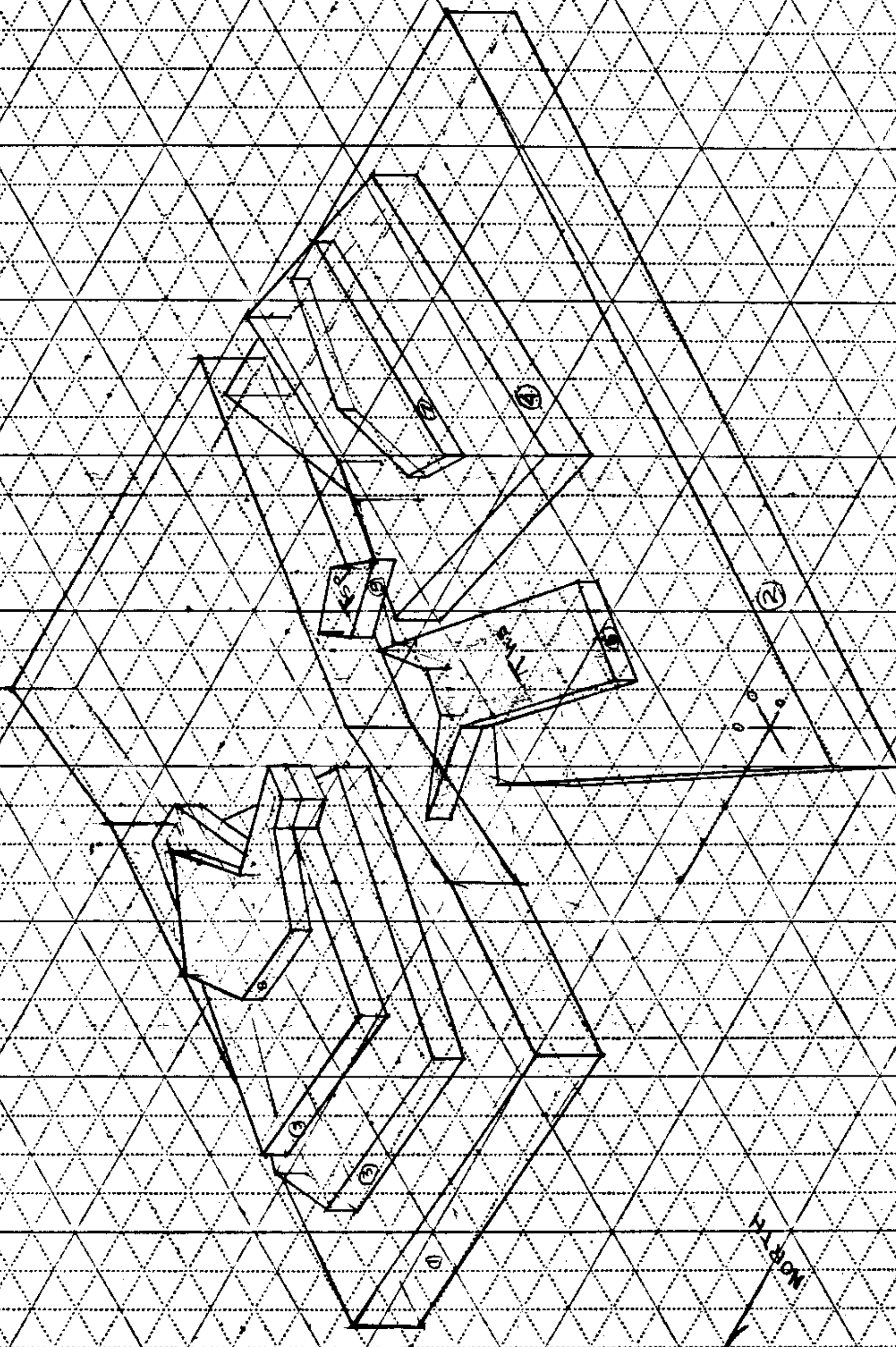

JOB-ID-BERKMAN /PROGRAM NAME:CALCON /PPNL27100,02700]/DATE AND TIME: 6-Mar-82 16:04

JOB-ID-BERKMAN /PROGRAM NAME:CALCON /PPNL27100,02700]/DATE AND TIME: 6-Mar-82 16:04

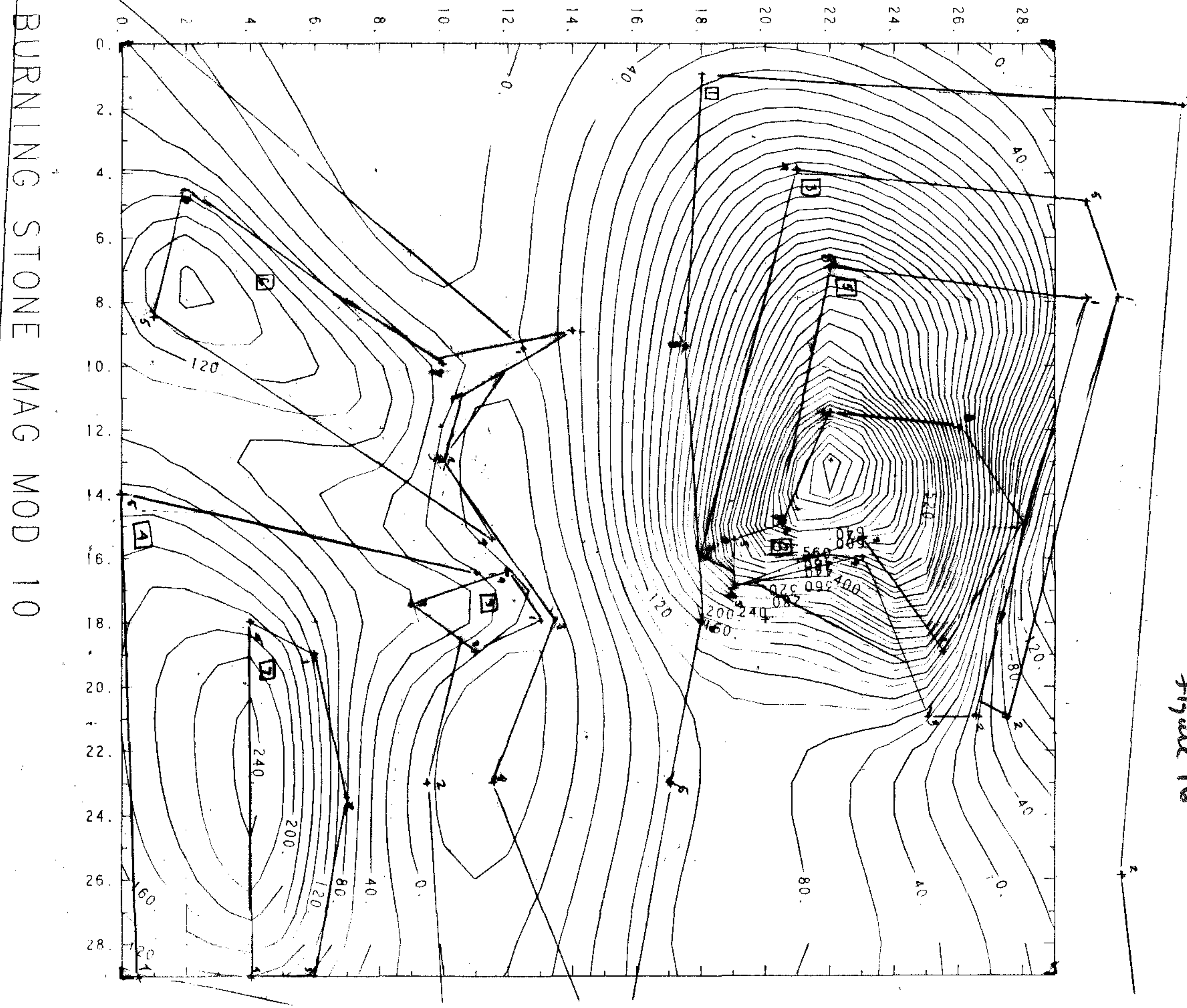

figure 16

JOB-ID:BERKMAN /PROGRAM NAME:CALCON /PPN[27100,02700]/DATE AND TIME: 6-Mar-82 16:06
JOB-ID:BERKMAN /PROGRAM NAME:CALCON /PPN[27100,02700]/DATE AND TIME: 6-Mar-82 16:06

BURNING STONE RES 10

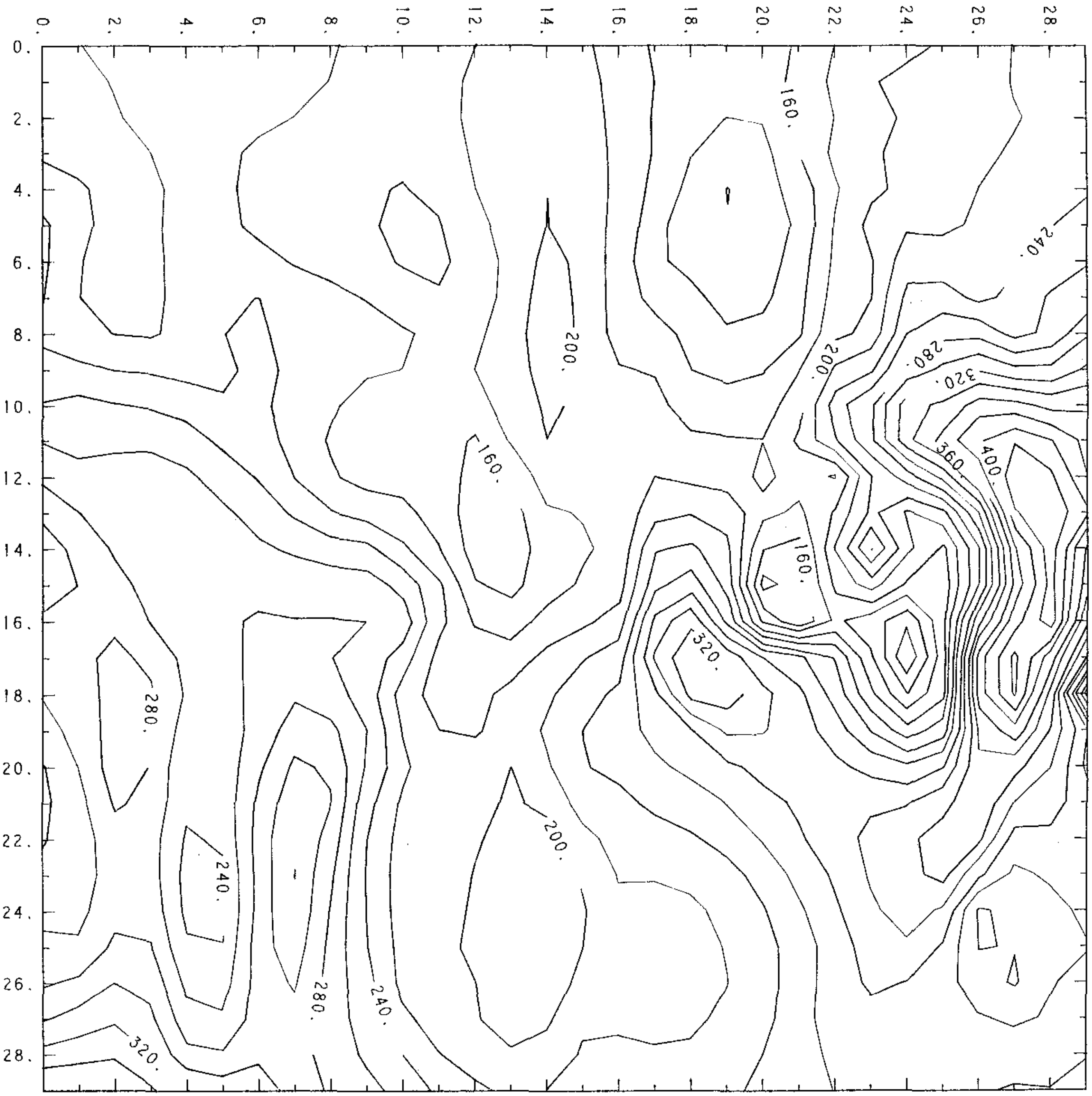

figure 17